PCCP

Cite this: *Phys. Chem. Chem. Phys.*, 2011, **13**, 13370–13381

www.rsc.org/pccp

PAPER

Nonionic diethanolamide amphiphiles with unsaturated C18 hydrocarbon chains: thermotropic and lyotropic liquid crystalline phase behavior†

Sharon M. Sagnella,[a] Charlotte E. Conn,[b] Irena Krodkiewska[b] and Calum J. Drummond*[b]

Received 3rd June 2011, Accepted 6th June 2011
DOI: 10.1039/c1cp21808e

The neat and lyotropic liquid crystalline phase behavior of three nonionic diethanolamide amphiphiles with C18 hydrocarbon chains containing one, two or three unsaturated bonds has been examined. This has allowed the effect of degree of unsaturation on the phase behavior of diethanolamide amphiphiles to be investigated. Neat linoleoyl and linolenoyl diethanolamide undergo a transition from a glassy liquid crystal to a liquid crystal at ~ -85 °C, while neat oleoyl diethanolamide undergoes a transition at ~ -60 °C to a liquid crystalline material before re-crystallizing at -34 °C. Oleoyl diethanolamide then undergoes a third transition from a crystalline phase to a smectic liquid crystalline phase at ~ 5 °C. In the absence of water, the transition temperature from a smectic liquid crystal to an isotropic liquid decreases with increasing unsaturation. The addition of water results in the formation of a lamellar phase (L_α) for all three amphiphiles. The lamellar phase is stable under excess water conditions up to temperatures of at least 70 °C. Approximate partial binary amphiphile-water phase diagrams generated for the three unsaturated C18 amphiphiles indicate that the excess water point for each amphiphile occurs at $\sim 60\%$ (w/w) amphiphile.

Introduction

Nonionic amphiphiles, such as surfactants, are integral components of many industrial and consumer products. Diethanolamide amphiphiles, and in particular those derived from lauric acid and coconut oil, have been widely used in the cosmetic industry, in a variety of household detergents, and more recently in an insecticide.[1–5] Their properties have additionally been exploited as foam boosters, thickening agents, and corrosion inhibitors.[1–7] Coconut oil, from which coconut diethanolamide is derived, consists of a range of both saturated fatty acid components (ranging from C6–C18) and unsaturated fatty acid components including monounsaturated oleic acid and polyunsaturated linoleic acid, thus coconut DEA contains diethanolamides of these different fatty acid components. While lauroyl diethanolamide has been studied in detail, physicochemical characterization of other coconut DEA components has been limited.

The unique physicochemical properties of the diethanolamide surfactants results from their amphiphilic nature; the hydrophilic headgroup can interact favorably with polar solvents while the hydrocarbon chains exhibit hydrophobic interactions. These interactions combined with local and global constraints dictated by shape, polarity, and molecular geometry drives the self-assembly of these molecules in the presence and absence of solvent.[8,9] For lyotropic phases, which are formed by amphiphiles in polar solvents such as water, the phase formed by the amphiphile can be explained with reference to the critical packing parameter ($CPP = \nu/(l_c a_0)$), where l_c is the effective length of an amphiphile chain, a_0 is the effective amphiphile headgroup area, and ν is the average volume occupied by the amphiphile chain.[9] "Rod-like" amphiphiles, where the molecule tends to be fairly cylindrical in shape and $\nu/(l_c a_0)$ has a value close to one, form flat bilayer structures. The fluid lamellar (L_α) phase consists of a one-dimensional stack of flat amphiphilic bilayers separated by water layers and is ubiquitous in nature as it forms the basic building block of biological membranes. However, for molecules where $\nu/(l_c a_0) < 1$, *i.e.* the headgroup area is large compared to that of the hydrocarbon chain, normal (oil in water) phases tend to form. Conversely inverse (water in oil) phases form when the hydrophobic chain occupies a larger volume than the head group, ($\nu/(l_c a_0) > 1$) thereby producing a molecule with an effective reverse wedge shape. As the effective reverse wedge-shape of the molecule increases, there is an increased desire for curvature of the interface resulting in the formation of inverse mesophases such as inverse bicontinuous cubic phases (Q_{II})[10] and the inverse

[a] *CSIRO Materials Science and Engineering, PO Box 184, North Ryde, NSW, 1670, Australia*
[b] *CSIRO Materials Science and Engineering, Bag 10, Clayton South, VIC, 3169, Australia. E-mail: Calum.Drummond@csiro.au*

† Electronic supplementary information (ESI) available: Polarized optical microscopy images of neat linoleoyl diethanolamide; Additional DSC heating scan of oleoyl diethanolamide with the different transition states indicated on the scan. See DOI: 10.1039/c1cp21808e

hexagonal phase (H_{II}).[11] An extremely high desire for curvature may result in the formation of inverse micelles where the hydrophilic headgroups are arranged towards water cores with hydrophobic chains radiating outwards. These micelles can be arranged in a disordered manner resulting in a fluid inverse micellar phase, the L_2 phase.[12]

The introduction of unsaturation into the hydrophobe has been shown to be an effective method of promoting the formation of inverse lyotropic phases in a variety of amphiphile families.[13–25] The most widely studied of the unsaturated amphiphile families is the monoacylglycerides, which have been shown to form a variety of non-lamellar phases including multiple inverse cubic phases and the inverse hexagonal phase highlighting the effect of chain length, degree of unsaturation and double bond positions on inverse phase formation.[13–15,19–21,23] Furthermore, unsaturated ethylene oxide amphiphiles containing a *cis* double bond form inverse bicontinuous cubic phases and an L_3 sponge phase.[18,24] Our group has previously examined in detail the structure-property correlation *via* modifications to the hydrophobe and headgroup of nonionic urea based surfactants demonstrating that unsaturation was one method for promoting inverse phase formation in this amphiphile family.[16,17,25–28] In addition, we and others have recently reported on the effect of hydrocarbon chain modification on the physicochemical properties of monoethanolamide amphiphiles demonstrating that hydrophobe unsaturation promotes inverse cubic phase formation within the monoethanolamide family.[22,29–31] Here, similar to the urea based amphiphiles, we have aimed to further extend our understanding of structure-property correlation of ethanolamide based amphiphiles by a systematic examination of the self-assembly, including neat and lyotropic liquid crystalline phase behavior of a series of C18 diethanolamides with one, two, and three carbon double bonds. Fig. 1 provides the chemical structures and compares the energy minimized structures of the previously examined unsaturated monoethanolamides,[30] as well as the unsaturated diethanolamide amphiphiles examined in the current study.

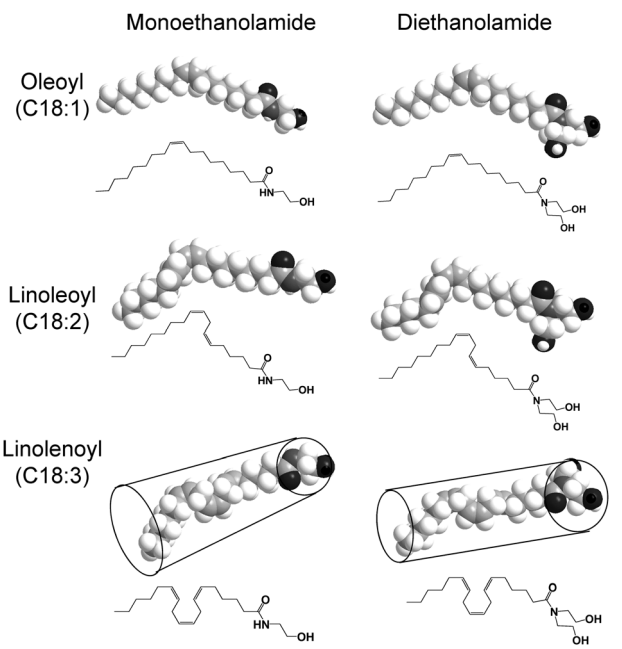

Fig. 1 Molecular models and chemical structures of unsaturated C18 mono and diethanolamide amphiphiles.

Experimental section

Materials

All reagents were obtained from Sigma-Aldrich. Organic solvents were either of analytical or spectroscopic grade and used as received. A Milli-Q Plus Ultrapure water system (Millipore; Australia) was used to filter deionized tap water to obtain high purity water.

Diethanolamide amphiphile synthesis

All diethanolamides reported in this paper were prepared by reaction of diethanolamine with the corresponding acid chloride. Diethanolamine (99.5% purity) was purchased from Fluka. Acid chlorides were formed from carboxylic acids, by using oxalyl chloride and catalytic dimethylformamide. The crude acid chlorides can be vacuum distilled but adequate purity can also be achieved by treatment with petroleum spirit (b.p. 30–40 °C), upon which most of the impurities separate as an insoluble oil. As an example, a detailed synthesis of oleoyl diethanolamide follows.

N,N-bis(2-hydroxyethyl)oleamide (*oleoyl diethanolamide*)

Step 1: ***Oleoyl chloride.*** 10 g (35.4 mmoles) of oleic acid (Sigma, 99% purity), 50 ml of dry dichloromethane and a small drop of DMF were placed in a 100 ml RB flask equipped with a dropping funnel, magnetic stirrer and air condenser under argon. The reaction flask was immersed in a water bath. A 2 M solution of 5.39 g (1.2 eq., 42.5 mmols) of oxalyl chloride in dry dichloromethane was added drop wise at room temperature (21 °C), and stirring was continued until all the acid had reacted as shown by NMR. The reaction mixture became pale yellow. Dichloromethane and excess of oxalyl chloride were removed on a rotary evaporator, and a light yellow crude oleoyl chloride was vacuum distilled, resulting in 10.08 g of a colorless liquid; 94.6% yield.

Step2: *Oleoyl diethanolamide* (*ODE*). The preparation of the amide is carried out in a two-necked 500-ml flask equipped with a magnetic stirrer, a thermometer and a pressure equalizing dropping funnel maintained in an argon atmosphere. Diethanolamine 14.12 g (4 eq.) was mixed into 150 ml of dry dichloromethane and cooled to −10 °C, not allowing the mixture to freeze. 10.08 g of oleoyl chloride (33.49 mmoles; 1 eq) diluted with 50 ml of dry dichloromethane was added drop wise, over 3 h. The temperature was initially −10 °C , and as the reaction was progressing, the temperature could be lowered to −30 and −40 °C. Stirring at this low temperature was continued for another hour, then the reaction mixture was left in the freezer until the next day. NMR of an aliquot taken at this point showed that the reaction was complete. In the freezer the excess of diethanolamine formed a solid upper layer. The flask was allowed to warm to room temperature, reaction mixture was transferred to a separatory funnel and cooled in the fridge to the point when the mixture separated into two clear phases: upper layer being an excess of diethanolamine. The DCM

phase was separated and washed with 10% NaCl aqueous solution; causing formation of an emulsion which was very slow to separate. For that reason DCM was evaporated off and the residue was redissolved in diethyl ether. NMR spectrum of this solution showed tiny amounts of impurities present in the material, therefore the etheral solution was further washed with 50 ml of 0.2N hydrochloric acid, followed by 40 ml of 2.5% KOH solution and finally with 50 ml water. Solvent was removed on rotary evaporator at room temperature, and the resulting colorless oil was further dried under vacuum. 9.34 g of a heavy colorless oil was obtained; yield 75.5%. HPLC anlaysis indicated that the purity of all three diethanolamide amphiphiles was >99%.

Oleoyl diethanolamide. ^{1}H NMR ($CDCl_3$, 400 MHz) δ 5.34, m, 2H, =CH; 3.87, t, *J* 4.9Hz, 2H, C$\underline{H}_2$OH; 3.79, t, *J* 5.1 Hz, 2H, C$\underline{H}_2$OH; 3.57, t, *J* 4.9 Hz, 2H, CH_2N; 3.51, t, *J* 5.3Hz, 2H, CH_2N; 3.08, br, 1H, OH; 2.87, br, 1H, OH; 2.39, t, *J* 7.7Hz, 2H, CH_2CO; 2.01, m, 4H, C$\underline{H}_2$CH=; 1.63, m, 2H, C$\underline{H}_2CH_2$CO; 1.22–1.38, m, 20H, CH_2; 0.88, t, *J* 6.8 Hz, CH_3.

Linoleoyl diethanolamide. ^{1}H NMR ($CDCl_3$, 400 MHz) δ 5.28–5.43, m, 4H, =CH; 3.87, t, *J* 4.8Hz, 2H, C$\underline{H}_2$OH; 3.79, t, *J* 5.1 Hz, 2H, C$\underline{H}_2$OH; 3.57, t, *J* 4.9 Hz, 2H, CH_2N; 3.50, t, *J* 5.3Hz, 2H, CH_2N; 3.12, br, 1H, OH; 2.93, br, 1H, OH; 2.77, t, *J* 6.6 Hz, 2H, =CHC$\underline{H}_2$CH=; 2.39, t, *J* 7.7 Hz, 2H, CH_2CO; 2.05, m, 4H, C$\underline{H}_2$CH=; 1.64, m, 2H, $CH_2C\underline{H}_2$CO; 1.24–1.41, m, 14H, CH_2; 0.89, t, *J* 6.9 Hz, 3H, CH_3.

Linolenoyl diethanolamide. ^{1}H NMR ($CDCl_3$, 400 MHz) δ 5.30–5.45, m, 6H, =CH; 3.87, t, *J* 4.9 Hz, 2H, C$\underline{H}_2$OH; 3.79, t, *J* 5.2 Hz, 2H, C$\underline{H}_2$OH; 3.57, t, *J* 4.9Hz, 2H, CH_2N; 3.50, t, *J* 5.3 Hz, 2H, CH_2N; 2.85–3.25, br, 2H, OH; 2.81, t, *J* 5.7 Hz, 4H, =CHC$\underline{H}_2$CH=; 2.41, t, *J* 7.6 Hz, 2H, CH_2CO; 2.00–2.15, m, 4H, C$\underline{H}_2$CH=; 1.67, m, 2H, C$\underline{H}_2CH_2$CO; 1.25–1.47, m, 8H, CH_2; 0.89, t, *J* 6.9 Hz, 3H, CH_3.

Differential scanning calorimetry (DSC)

DSC was performed using a Mettler DSC822^e system with a Mettler TSO 801RO sample robot (Mettler Toledo; Melbourne, Australia). Samples were run at scan rates of 10 and 2.5 °C/min and collected using the STARe software package (Mettler Toledo; Melbourne, Australia). Temperature calibration (±0.3 °C) of the ceramic sensor was performed using octane, water, indium, and zinc. Integration of a standard indium peak was used for thermal calibration. The energies and peak temperatures of the endotherms/exotherms of the diethanolamide amphiphiles were determined using the STARe software package.

X-ray diffraction (XRD)

XRD analyses were performed on a PANalytical X'pert PRO X-ray diffractometer. Incident X-ray radiation was produced from a line-focused PW3373/00 Cu X-ray tube operating at 45 kV and 40 mA. The solid sample was placed and pressed into a circular metal sample. The sample stage was Spinner PW3064 with reflection but not moving. The diffracted beam produced by interaction with the sample was detected by an X'Pert data collector. Samples were analyzed at room temperature over a range of 2–60° 2θ with a step size of 0.05° 2θ, with each step measured for 60 s. The raw data was exported and plotted in Microsoft Excel as q value (nm^{-1}) *vs.* intensity. The q value (nm^{-1}) was calculated from 2θ based on Bragg's law ($\lambda_{Cu-K\alpha}$ = 0.154 nm).

Water penetration into diethanolamide amphiphiles

A small amount of neat diethanolamide amphiphile was placed onto a microscope slide and heated to melting. A coverslip was placed on top of the melted amphiphile and then cooled to room temperature prior to addition of water. Water placed at the edges of the coverslip was drawn between the two glass surfaces to surround the "solidified" material by capillary action. The microscope slide was placed into a Linkam PE94 hot stage (Linkam Scientific Instruments Ltd; Surry, England) and heated at 1 °C/min or less. The interaction of water and the monoethanolamide amphiphile was observed with an Olympus GX51 inverted optical microscope (Olympus Australia Pty. Ltd.; Melbourne, Australia) in the presence and absence of crossed polarizing lenses. Images were captured with an Olympus c-5060 digital camera (Olympus Australia Pty. Ltd.; Melbourne, Australia).

Binary phase behavior of diethanolamide amphiphiles

Diethanolamide amphiphile–water mixtures were prepared by weighing out an amount of the diethanolamide amphiphile in glass ampoules, and then adding the necessary quantity of water by weight. Samples ranging from 5 wt% amphiphile in water to 95 wt% amphiphile in water were prepared. The glass ampoules were sealed, and the amphiphile was initially dissolved (as much as possible) by heating the samples followed by rapid cooling. Samples were then submerged into a glass water bath with crossed polarizing film attached to the outside of the water bath. The water temperature was controlled and monitored by a polystat cc1 water bath heater (Crown Scientific Pty. Ltd.; Sydney, Australia) equipped with an internal digital thermometer. The temperature was incrementally increased and then left to allow the samples to equilibrate properly. Samples were illuminated and examined through the cross polarizing filters to determine phase transitions.

SAXS

Samples for SAXS analysis were prepared by weighing approximately 50 mgs of lipid into a vial and adding the appropriate amount of deionised water by weight. Samples were then re-weighed so the water content could be calculated accurately. Samples were partially homogenized by using a mechanical vortex but this did not fully homogenize the samples. It is common to homogenize a binary lipid-water sample by heating to fluidity then cooling to room temperature; however, in this case, heating was avoided due to the labile nature of the chemicals. After one week equilibration, samples were still visually inhomogeneous and were therefore stirred vigorously with a spatula prior to SAXS measurements being taken. All SAXS measurements showed sharp diffraction peaks consistent with homogeneous samples.

SAXS measurements were carried out using the SAXS/WAXS beamline at the Australian Synchrotron. The experiments

used a beam of wavelength $\lambda = 1.24$ Å (10.00 keV) with dimensions 700 μm × 500 μm and a typical flux of 1.2×10^{13} photons/s. 2-D diffraction images were recorded on a Pilatus 1M detector, which offers very low noise, a large dynamic range and rapid data collection over a large active area. Dead space due to intermodule gaps is overcome by radial integration with the detector slightly offset. Calibration of the q-axis of the 1-D diffraction patterns was performed using silver behenate as standard.

Liquid crystalline mesophases give rise to distinct diffraction patterns which may be used as an unambiguous identification for each phase, provided an adequate number of reflections are observed. All images were analyzed using AXcess, a custom-built SAXS analysis program written by Dr Andrew Heron: details on the use of AXcess for SAXS analysis are reported in a review article.[32]

Molecular modeling

Chem 3D pro v11 (Cambridgesoft Corporation) was used to obtain the energy minimized conformation using its MM2 energy minimization routine as well as theoretical molecular lengths. This software package ceases optimization at local minimums. Therefore, when a change from linearity occurred, bonds were rotated manually, and minimization was continued. Thus, an optimum energy minimum conformation was obtained. Molecular lengths were measured from the minimized conformations as the longest distance between the end of the hydrocarbon chain and the furthest atom in the diethanolamide headgroup.

Results and discussion

Thermal behavior of unsaturated diethanolamide neat amphiphiles

DSC scans were run at 2.5 °C/min (Fig. 2) and 10 °C/min (not shown) for all three unsaturated diethanolamide surfactants. DSC scans run at 10 °C/min were started at −130 °C, and no additional peaks were observed at temperatures below those shown. To ease visualization of low enthalpy transitions, the curves of linoleoyl and linolenoyl diethanolamide, as well as oleoyl diethanolamide at temperatures above 10 °C, have been magnified x10 and are shown in Fig. 2B. Multiple heating/cooling cycles were performed for each sample in order to resolve any polymorphisms in the sample. Analysis of the DSC curves to determine transition temperatures and their associated enthalpies is provided in Table 1. Phase transition temperatures are reported as the peak maxima of the appropriate endo- or exotherm. Enthalpies were obtained by integration of the transition peaks.

The melting transition temperature has been plotted as a function of the degree of unsaturation for the C18 diethanolamide amphiphiles in Fig. 3.[25,26,30,33–36] Literature values for the corresponding fatty acids, ureas, amides, alcohols, monoglycerides, and monoethanolamides have been plotted on the same graph for comparison. The melting temperature of C18 amphiphiles with different polar head groups follows the general trend: ureas > amides > monoethanolamides > monoglycerides ≈ diethanolamides > fatty acids > alcohols.

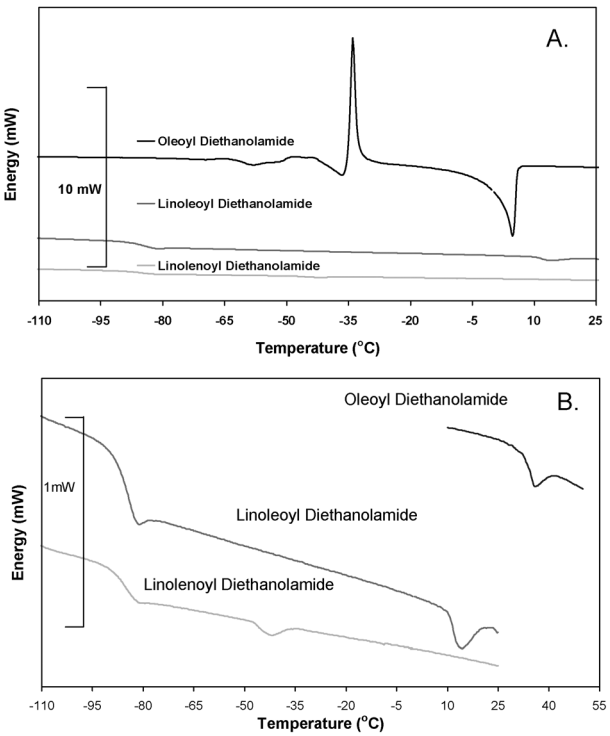

Fig. 2 Differential Scanning Calorimetry of oleoyl diethanolamide, linoleoyl diethanolamide and γ-linolenoyl diethanolamide. (A). Scan Rate 2.5 °C/min, (B). Scan Rate 2.5 °C/min, enthalpy x10 to resolve low energy transitions.

This trend changes slightly for the C18 amphiphiles with three unsaturated bonds (Fig. 3). The amides and ureas have the highest melting points due to the strong H-bonding network within the headgroups of these amphiphiles.[16,25–28] As the degree of unsaturation is increased, the decrease in melting points of these C18 amphiphile families tends to level out. A similar trend is observed for the fatty acids and alcohols, which have much lower melting points than the amides and ureas. In contrast, the melting points of the diethanolamide amphiphiles, the monoethanolamides amphiphiles[30] and the monoglycerides display a more linear dependence on the degree of unsaturation. We note that the melting points of the C18 diethanolamide amphiphiles are almost identical to their monoglyceride counterparts. This is most likely due to the close similarities in molecular structure of the diethanolamides and the monoglycerides, which results in a similar degree of headgroup H-bonding.

In terms of thermal behavior, one of the main differences between the unsaturated C18 diethanolamides and their monoethanolamide counterparts is that while the monoethanolamides all exhibit a distinct crystal-isotropic transition,[30] the unsaturated diethanolamides instead undergo an extremely low enthalpy transition (C18:1, 37.5 °C; C18:2, 20 °C;.C18:3, −47 °C). These low enthalpy transitions may be attributed to the transition from a liquid crystal to an isotropic fluid, also called the clearing point. The presence of a clearing point for the neat amphiphile has also been observed for the H-farnesoyl and phytanoyl monoethanolamide and urea amphiphiles as well as certain alkyl glucosides.[26,29,37]

Table 1 Thermal transition for unsaturated C18 diethanolamide amphiphiles determined from DSC scanned at 2.5 °C/min

	Glass Transition Temp (°C)	Smectic LC–Isotropic Melting Temp (°C)	Smectic LC–Isotropic Melting Enthalpy (kJ/mol)	Devitrification Temp (°C)	Devitrification Enthalpy (kJ/mol)	Crystal–Smectic LC Melting Temp (°C)	Crystal–Smectic LC Melting Enthalpy (kJ/mol)
Stearoyl Diethanolamide[62] (C18:0)[a]	—	—	—	—	—	73.4 ± 0.2[b]	66.2 ± 2.4[b]
Oleoyl Diethanolamide (C18:1)	−60.4 ± 0.3	39.9 ± 3.4	−0.22 ± 0.2	−34.3 ± 0.6	11.7 ± 0.4	(−21.8)[a], 5.3 ± 0.7	(−6.5)[a], −19.2 ± 6.2
Linoleoyl Diethanolamide (C18:2)	−85.7 ± 0.6	19.9 ± 8.3	−0.3 ± 0.2	—	—	—	—
γ-Linolenoyl Diethanolamide (C18:3)	−87.2 ± 3.2	−46.7 ± 6.2	−0.25 ± 0.02	—	—	—	—

[a] crystal-crystal transition (data obtained from Fig. S2, ESI†). [b] crystal-isotropic liquid melting.

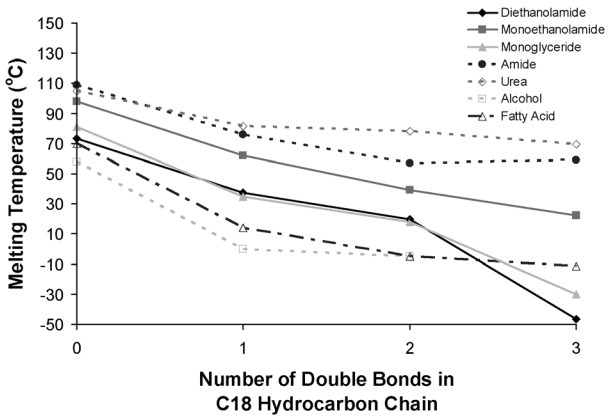

Fig. 3 Melting behaviour of unsaturated C18 amphiphiles with different headgroups.

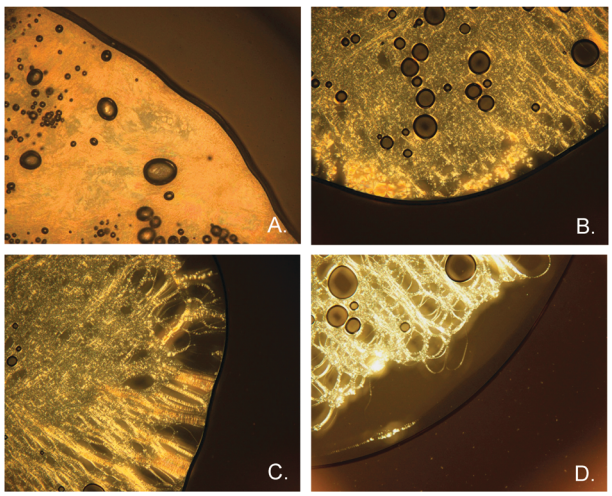

Fig. 4 Polarized optical microscope images of neat oleoyl diethanolamide. A. Image acquired at 5 °C showing a crystalline solid, B. and C. Image acquired at 30 °C showing typical smectic liquid crystalline texture. D. Image acquired at 35 °C, an isotropic band is present at the edge of the amphiphile indicating melting of the liquid crystalline phase to a fluid isotropic phase. These transitions occur at similar temperatures to the transitions indicated by DSC (mag 100x).

A combination of SAXS and polarized optical microscopy measurements were carried out on the neat oleoyl (Fig. 4) and linoleoyl (Fig. S1, ESI†) diethanolamide amphiphiles at different temperatures, to confirm the existence of a liquid crystalline phase. The data indicate the formation of a layered smectic liquid crystal for both samples and are described in detail in subsequent sections. Similar data were not obtained for linolenoyl diethanolamide as the liquid crystal–isotropic fluid transition for this amphiphile occurs at sub-zero temperatures. As the temperature is increased above the clearing point, both oleoyl (Fig. 4D) and linoleoyl (Fig. S1B, ESI†) diethanolamide begin to become an isotropic melt, as demonstrated by the dark isotropic band at the edge of the amphiphile. Upon standing at these temperatures for 10 min, the liquid crystalline phase transitions fully to an isotropic melt (not shown).

The smectic liquid crystalline phase consists of a stack of lipid bilayers with hydrophilic headgroups sandwiched between the hydrophobic tails. It is similar in structure to the hydrated lyotropic fluid lamellar (L_α) phase but without the water layers. In both cases the formation of the bilayer structure acts to shield the hydrophobic hydrocarbon chains from unfavorable interactions with either the hydrophilic headgroups or, in the case of the fluid lamellar phase, with a polar solvent. As described in the introduction the formation of this type of structure is common for "rod-like" amphiphiles.[8,38–40] As shown in Fig. 1, the diethanolamide headgroup occupies a much larger area than the monoethanolamide headgroup thus resulting in a more cylindrical molecular geometry which favors smectic liquid crystalline formation.

Another unique thermal property of the unsaturated diethanolamides is that all three exhibit a glass transition temperature. This transition occurs at almost identical temperatures (~−85 °C) for the linoleoyl and linolenoyl diethanolamide and at a higher temperature (−60 °C) for oleoyl diethanolamide. Glass transitions, while commonly seen in polymers, are not as common

in amphiphiles. Due to the size and complexity of polymers, in most cases they are unable to form crystals and instead their polymer chain motion ceases below their T_g becoming an amorphous solid or glass. We have noted the presence of glass transition temperatures in isoprenoid-type amphiphiles containing both monoethanolamide and urea headgroups at temperatures ranging from −72 to −77 °C[26,29] and in phytantriol at ∼−40 °C (unpublished data). In addition, phytanyl and farnesyl ethylene oxide, mono and bis-phytanyl EDTA, certain endogenous arachidonyl chained amphiphiles, thymidine phytanyl, 5FC-phytanyl, and some n-alkyl maltosides exhibit glass transitions.[41–50]

Unlike crystals, amorphous solids lack long range translational order. In the case of the amphiphiles mentioned above, however, instead of forming an amorphous solid, below their T_g they form a glassy liquid crystal.[26,29,46,40–42] A glassy liquid crystal is one in which the glass possesses the same structure as its corresponding liquid crystal, but molecular motion is "frozen." The ability of an amphiphile to form a glassy liquid crystal is reliant on extensive H-bonding within the headgroup. Typically, these types of amphiphiles first undergo an initial low temperature transition from a glassy state to one or more liquid crystalline states, before finally becoming an isotropic fluid at the molecule's clearing point, however, we have noted that the DSC and POM data suggests that this type of direct transition does not in fact occur for oleoyl diethanolamide.

Despite the fact that oleoyl diethanolamide forms a glassy liquid crystal, it does not transition in a direct manner from glassy liquid crystal–liquid crystal–isotropic fluid upon heating, but instead undergoes devitrification, or crystal formation at −34 °C followed by liquid crystal formation at 5 °C. Thus, oleoyl diethanolamide undergoes the following transition order: glassy liquid crystal–liquid crystal–crystalline–liquid crystal–isotropic fluid. In addition, in the first heating scan of the oleoyl diethanolamide sample (Fig. S2, ESI†), an additional crystalline pre-transition is present that occurs after the devitrification peak and before the main crystalline melting point, and can be attributed to a crystal-crystal transition. This pre-transition is highly dependent on the sample history and disappears in subsequent heating scans. Similar polymorphic crystal transitions occur in oleoyl monoethanolamide.[30] Pure oleic acid displays a single pre-transition which has been ascribed to a well characterized polymorphic transition from the γ- to α-form. The difference between the two forms has to do with the conformation of the section of the hydrocarbon chain between the double bond and the terminal methyl group which retains an all trans structure in the γ-form, while possessing a disordered liquid like conformation in the α-form.[51–53]

XRD of neat unsaturated diethanolamide amphiphiles

A typical 1-D X-ray powder diffraction pattern, for neat oleoyl diethanolamide at 25 °C, is shown in Fig. 5. Two low-angle peaks are observed at q-values of 1.83 and 3.65 nm^{-1}, consistent with the first and second order reflections of a lamellar phase of lattice parameter 34.4 Å. For linoleoyl diethanolamide a single distinct low angle peak was observed at a q-value of 1.90 nm^{-1} close to the low-angle resolution of the beamline

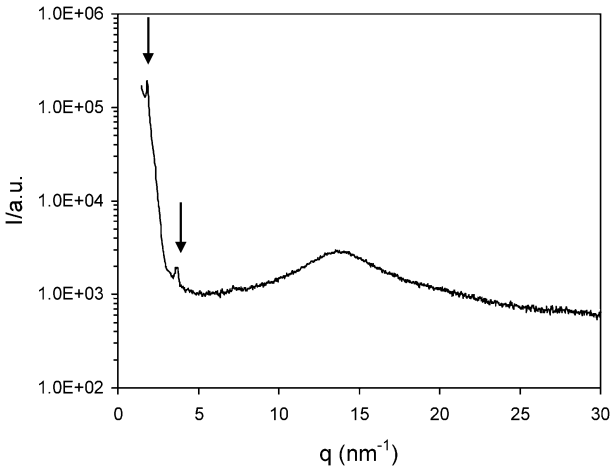

Fig. 5 1-D XRD plot of intensity *vs.* q for neat oleoyl diethanolamide. The first and second order reflections of a lamellar phase are indicated. A broad peak in the wide angle region is indicative of disordered hydrocarbon chains.

(data not shown). Based on comparison with POM results we suggest this represents the first-order reflection of a lamellar phase of d-spacing 33.0 Å. The presence of this lamellar phase was confirmed by SAXS analysis of the neat sample and is discussed in detail in a later section. In both cases the XRD patterns display a broad peak centered around a q-value of ∼14 nm^{-1} (*ca.* 4.5 Å) indicative of fluid hydrocarbon chains[41,42,54] In contrast, "gel-like" lamellar phases, *i.e.* where the chains are packed into an all-trans configuration but the headgroups are disordered, show a narrow, well defined peak at *ca.* 4.2 Å that is typical for packed, all-trans alkyl chains.[41,55] Crystalline chain packing leads to many well-defined peaks in this region. Thus, the broad peak is attributed to the unsaturated chains residing in a disorganized or molten state, while the distinct reflections in the low angle region arise due to the long-range layered lamellar structure of the amphiphile molecules.[41,42,54,55]

Due to increased chain splay associated with unsaturated hydrocarbon chains, the theoretical length of unsaturated hydrocarbon chains will be less than that predicted *via* Tanford's formula. Theoretical molecular lengths were therefore obtained *via* molecular modeling from energy minimized structures of the amphiphiles. The theoretical length of one oleoyl diethanolamide molecule was determined to be 24.7 Å (d = 49.4 Å), while for linoleoyl diethanolamide it was 22.2 Å (d = 44.4 Å). We note that both the predicted and measured lengths of the linoleoyl derivative are slightly shorter than those for its oleoyl counterpart, reflecting the increased degree of unsaturation of the linoleoyl chain, which results in an effective shortening of the alkyl chain. The d-spacing obtained by XRD for both linoleoyl and oleoyl diethanolamide is significantly less than the predicted d-spacing for non-tilted and non-interdigitated bilayers. Similar results have been demonstrated for carbohydrate amphiphiles in which the measured d-spacing is typically ∼1.3–1.4 times the predicted length of a monolayer, and in diols where the difference is ∼1.6–1.7 times the predicted length.[41,42,54] For alkylglucosides/maltosides, the difference in measured *versus* predicted distance is accounted for by partial interdigitation of the alkyl chains, although in

some cases tilting also occurs.[41,42,56] With the diols, the alkyl chains are in an extremely disordered state, and thus little interdigitation occurs. Instead, H-bonding in the diol headgroups is responsible for smectic layer formation, with disordered chains sandwiched between the ordered headgroups. The extremely disordered chains combined with a predicted tilt account for the difference in measurements for this class of amphiphiles.[54] It has been demonstrated that the alkyl chain length is reduced ~20% in the disorganized liquid crystalline phase.[42,57] In the case of the unsaturated diethanolamides, the location of the two OH moieties in the headgroup is similar to that of the diols and thus it is likely a similar smectic liquid crystalline structure occurs in these amphiphiles as predicted for the diols thus resulting in the difference between the measured length and predicted length of the amphiphiles. However, further structural studies are necessary in order to fully describe the exact structure of the smectic liquid crystalline phase.

Lyotropic phase behavior of unsaturated diethanolamide amphiphiles

Cross-polarized light microscopy (POM) was used to provide a simple and rapid assessment of the lyotropic phase behavior of the three unsaturated diethanolamide amphiphiles, Fig. 6. Under cross polarizers, cubic and micellar phases appear as dark bands while anisotropic phases such as lamellar and hexagonal phases are birefringent with well characterized textures.[58] The sequence of phases formed from the water/amphiphile interface along with their evident viscosity and texture formation provide circumstantial evidence for phase identification. Amphiphile/water mixtures ranging from 5 wt% water to 95 wt% water were then made in sealed ampoules and examined over a range of temperatures to construct a preliminary partial binary phase diagram. SAXS experiments were run at various concentrations sampling the region of interest determined from the partial binary phase diagram in order to provide definitive phase assignment and lattice parameters.

POM measurements indicated that all three unsaturated diethanolamides form self-assembly phases in water. The phase behavior observed for all three compounds was quite similar with each forming an L_α phase in excess water over a large temperature range. The temperature range over which the lamellar phase was observed for each diethanolamide are presented in Table 2.

The presence of a fluid lamellar phase was confirmed by SAXS measurements, Fig. 7, and lattice parameters are presented as a function of water content and temperature in Fig. 8.

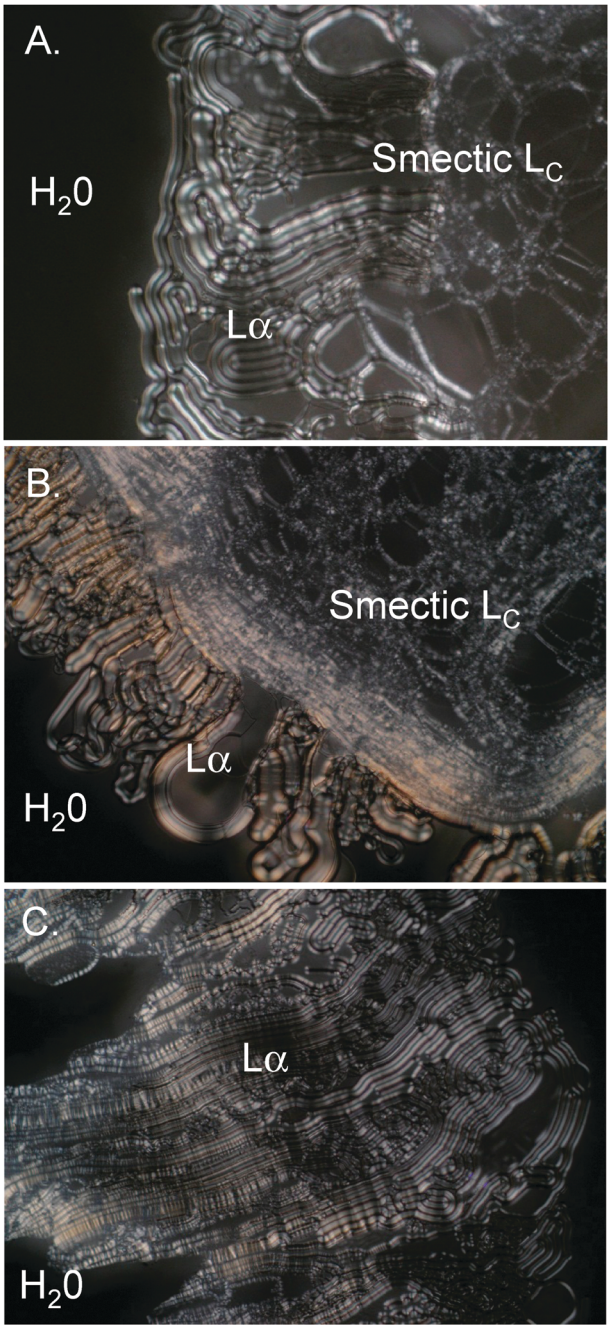

Fig. 6 Polarized optical microscope images of water penetration of A. oleoyl diethanolamide, B. linoleoyl diethanolamide, and C. linolenoyl diethanolamide All images were acquired at 25 °C (mag 100x).

Oleoyl diethanolamide

Initial water penetration scans using cross-POM indicated that oleoyl diethanolamide forms an L_α phase at ~5 °C, stable up to 85 °C, Fig. 6A. In addition to the L_α phase, the neat surfactant resides as a smectic liquid crystal. The smectic liquid crystalline phase melts around 37 °C to form an isotropic liquid phase in addition to the lamellar phase. Above 85 °C, the entire amphiphile/water mixture becomes an isotropic melt. An approximate partial binary phase diagram of oleoyl diethanolamide was constructed from samples with a controlled water content ranging from 5 wt% water to 95 wt% water sealed in glass ampoules allowing approximate phase boundaries in both composition and temperature to be defined as shown in Fig. 9A. Below 5 °C the system adopts a fully crystalline phase at all water compositions studied. Above this temperature the system was anisotropic at all water contents consistent with the formation of a lamellar phase. A fluid isotropic phase begins to form at low water contents at temperatures above 37 °C. The excess water point for the L_α phase is approximately 40 wt% water.

SAXS experiments were therefore carried out to allow definitive phase assignments to be made. Experiments, using

Table 2 Phases observed *via* optical microscopy, and the temperatures at which they appear. All three unsaturated C18 diethanolamides form an L_α phase in excess water at room and physiological temperature

Amphiphile	Lamellar	Hexagonal	Isotropic	Isotropic Melt
Stearoyl Diethanolamide (C18:0)[b]	55–75 °C	—	—	75 °C
Oleoyl diethanolamide (C18:1)	5–85 °C	—	—	85 °C
Linoleoyl diethanolamide (C18:2)	15–75 °C	—	—	75 °C
γ-linolenoyl diethanolamide (C18:3)	5–70 °C[a]	—	—	70 °C

[a] Not examined below this temperature. [b] Saturated C18 Diethanolamide data added for comparison.[62]

the SAXS/WAXS beamline at the Australian Synchrotron, were run on oleoyl ethanolamide samples at 0, 5, 10, 20, 30 and 50 wt% H_2O and at temperatures between 10 and 70 °C. A typical 1-D diffraction pattern for oleoyl di-ethanolamide (10 wt% water) at 20 °C is shown in Fig. 7A, Four reflections in the ratio 1 : 2 : 3 : 4 are observed, marked with an asterisk in Fig. 7A, consistent with the formation of a lamellar phase. A diffuse peak was also observed in the wide-angle region at a q-value of 4.5 $Å^{-1}$ indicative of fluid hydrocarbon chains. The combined phase diagram, showing results from POM and SAXS is shown in Fig. 9(A). In general we note good agreement between SAXS and POM experiments with a fluid lamellar phase observed for all samples studied.

The lattice parameter of the fluid lamellar phase is plotted in Fig. 8A as a function of water content, at 10, 20 and 37 °C. A significant increase in the lattice parameter with increased water content is observed, consistent with water uptake by the fluid lamellar phase. In addition there is a small decrease in lattice parameter with increasing temperature, reflecting increased chain splay at higher temperatures. The observed decrease in lattice parameter with temperature is significantly greater under excess water conditions (50 wt% water) than under limited hydration conditions ($\leq$30 wt% water). This may reflect the increased constraint on hydrocarbon chain movement under limited hydration conditions, preventing the chains from adopting their preferred conformation.

Linoleoyl diethanolamide

Initial water penetration scans using cross-POM indicated that linolenoyl diethanolamide forms an L_α phase at ~15 °C which is stable up to 75 °C (Fig. 6B). In addition to the L_α phase, the neat surfactant resides as a smectic liquid crystal. The smectic liquid crystalline phase melts around 25 °C to form an isotropic liquid phase in addition to the L_α phase. Above 75 °C, the entire amphiphile/water mixture becomes an isotropic liquid. A partial binary phase diagram of linolenoyl ethanolamide was constructed from samples with a controlled water content ranging from 5 wt% water to 95 wt% water sealed in glass ampoules, allowing approximate phase boundaries in both composition and temperature to be defined as shown in Fig. 9B. SAXS experiments were then carried out on samples at 0, 20, 30 and 50 wt% water at temperatures between 10 and 70 °C. The combined phase diagram, showing results from POM and SAXS is shown in Fig. 9B.

The phase behavior of linoleoyl diethanolamide is similar to that of oleoyl diethanolamide with the formation of a smectic phase for the neat sample and a fluid lamellar phase in the presence of water. A typical 1-D diffraction pattern, for linoleoyl di-ethanolamide (30 wt% water) at 20 °C, is shown in Fig. 7B The first and second order reflections of a lamellar phase are marked with an asterisk. Again a diffuse peak in the wide-angle region is indicative of a fluid lamellar phase. We note that the fluid micellar L_2 phase observed at low water contents (< 5 wt%) and at temperatures > ~25 °C by POM, was not observed using SAXS.

The lattice parameter of the lamellar phase formed by linolenoyl di-ethanolamide is shown in Fig. 8B as a function of water content at 10, 20, 25 and 37 °C. As for oleoyl di-ethanolamide we note that the lattice parameter of the fluid lamellar phase increases significantly with increasing water content and decreases with increasing temperature.

Linolenoyl ethanolamide

Initial water penetration scans using cross-POM indicated that linolenoyl diethanolamide forms an L_α phase at all temperatures examined, which is stable up to 70 °C (Fig. 6C). Above 70 °C, the entire amphiphile/water mixture becomes an isotropic melt. A partial binary phase diagram for linolenoyl ethanolamide was constructed from samples with a controlled water content ranging from 5 wt% water to 95 wt% water sealed in glass ampoules, allowing approximate phase boundaries in both composition and temperature to be defined as shown in Fig. 9C. The phase behavior of linolenoyl diethanolamide is similar to that of the other two amphiphiles at temperatures well above their smectic liquid crystalline melting temperatures. At low water contents ($\leq$10 wt% water) the system is fluid isotropic at all temperatures examined, while at water contents above this, the entire system forms an L_α phase. As with the other two amphiphiles, the excess water point for the L_α phase is approximately 40 wt% water.

As linolenoyl diethanolamide is particularly unstable, SAXS experiments were only carried out on a sample under excess water conditions. Experiments were carried out at the Australian Synchrotron at 25, 50 and 70 °C. A typical diffraction pattern, at 25 °C is shown in Fig. 7C. The calculated lattice parameter is 45.4 ± 0.1 Å (25 °C), 42.9 ± 0.1 Å (50 °C), and 41.7 ± 0.1 Å (70 °C), again displaying a decrease with increasing temperature.

Structure-property comparisons

Unlike the unsaturated C18 monoethanolamides which possess an effective wedge-shaped conformation due to the small headgroup and relatively large volume occupied by the hydrocarbon chains resulting from the chain splay introduced *via* unsaturation[30] the unsaturated C18 diethanolamide molecules effectively possess a more rod-like or cylindrical conformation due to the larger area occupied by the diethanolamide headgroup (Fig. 1). This effective molecular geometry has been shown to

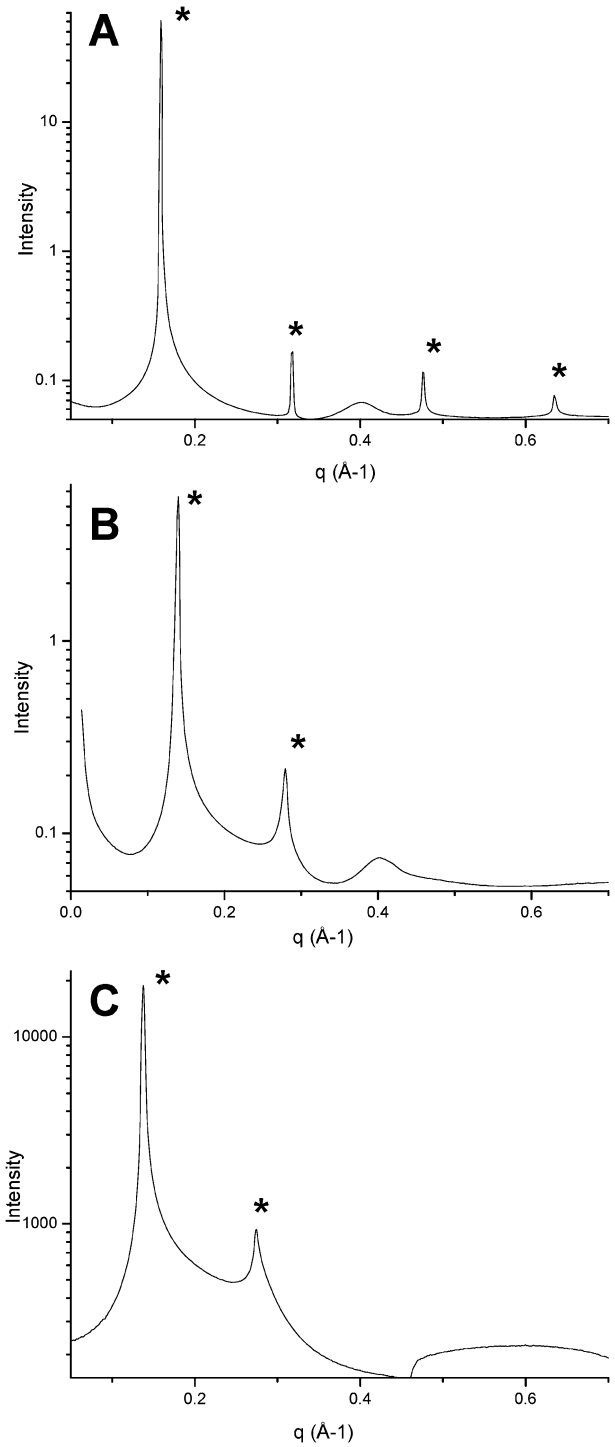

Fig. 7 1-D SAXS plots of intensity *vs.* q for A. oleoyl diethanolamide (10 wt% water), B. linoleoyl diethanolamide (30 wt% water) and C. linolenoyl diethanolamide (50 wt% water). A and B were run at 20 °C and C at 25 °C. In A the first, second, third and fourth order reflections of a lamellar phase are observed. In B and C the first and second order reflections of a lamellar phase are indicated. A broad peak observed at a q-value of approximately 0.4 $Å^{-1}$ in A and B is a kapton signal from the kapton tape used to contain the samples within the paste cell.

favor the formation of both lyotropic lamellar phases and thermotropic smectic liquid crystal phases.

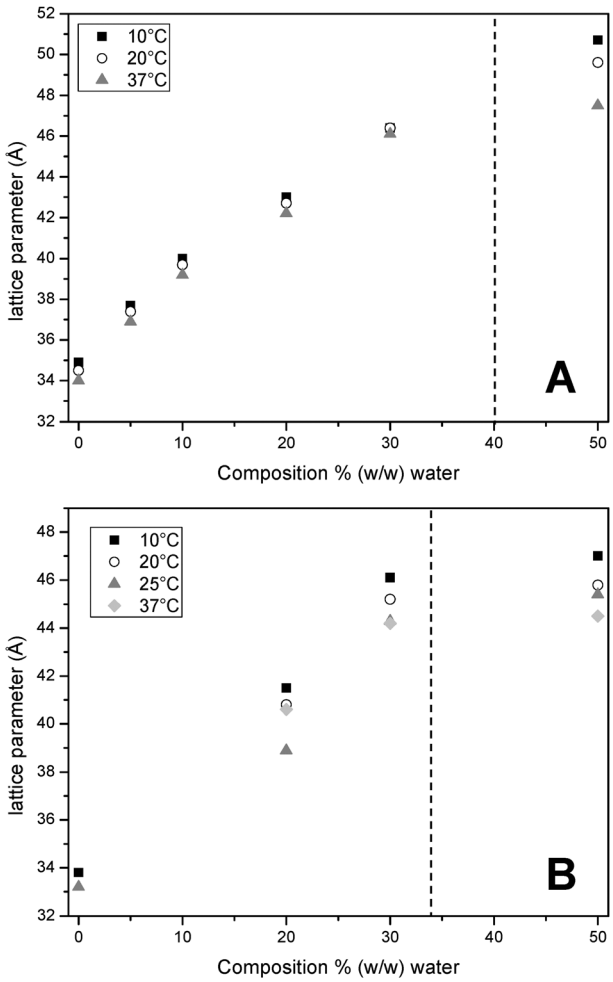

Fig. 8 The lattice parameter of the lamellar phase is plotted as a function of water content for A. oleoyl diethanolamide and B. linoleoyl diethanolamide. Data are shown at a range of temperatures between 10 and 37 °C. In both cases the approximate excess water point is marked by a dashed line.

Molecules that can form both thermotropic and lyotropic liquid crystalline phases are known as amphitropic compounds. In the case of non-ionic amphitropic amphiphiles, polyhydroxy and carbohydrate amphiphiles are the most widely investigated compounds exhibiting this property.[37,59] The diethanolamide headgroup is one of the simplest examples of a polyhydroxy headgroup consisting of two terminal –OH moieties. The presence of the two hydroxyl groups in addition to the amide linkage connecting the diethanolamide headgroup to the unsaturated alkyl chain allows for extensive intermolecular H-bonding among headgroups. The formation of smectic phases in polyhydoxy and carbohydrate amphiphiles has been attributed to extensive intermolecular H-bonding networks between headgroups. The alkyl chains are described as being sandwiched between the headgroup network.[42,56,57,59,60] In all cases the d-spacing corresponds to $l < d < 2l$, where l is the length of the fully extended molecule and d is the bilayer thickness. This result holds true for the unsaturated diethanolamide amphiphiles as well. Thus, the multiple hydroxyl groups combined with the XRD and SAXS data support a smectic bilayer structure for this class of amphiphiles with

disorganized interdigitating alkyl chains at the core. The transition between thermotropic and lyotropic phases for this family of molecules should be continuous since they are non-ionic and thus the addition of water will not significantly alter the intermolecular H-bonding.[59] Thus, the addition of water sees the smectic liquid crystal phase of the unsaturated diethanolamides transition to a fully swollen lyotropic lamellar liquid crystal phase. The one difference that occurs with the addition of water is that it imparts a greater degree of thermal stability to the H-bonding network thus allowing stabilization of the L_α phase up to much higher temperatures than the smectic liquid crystalline phase.

As the degree of unsaturation increases the lattice parameter of the fully swollen fluid lamellar phase decreases. For example, at room temperature all three diethanolamide amphiphiles adopt a fluid lamellar phase with lattice parameters of 49.6 Å (20 °C), 45.4 Å (25 °C) and 42.9 Å (25 °C) for oleoyl, linoleoyl and linolenoyl di-ethanolamide respectively. This reflects the increased 'kinking' introduced into the chain with higher degree of unsaturation which acts to increase chain splay and hence reduce the bilayer thickness.

The temperature at which the L_α phase eventually becomes fluid isotropic also increases linearly with decreasing degree of unsaturation. Similarly, the temperature at which the smectic liquid crystalline phase melts to a fluid isotropic phase increases somewhat linearly with a decreasing degree of unsaturation. These results indicate that the chain splay introduced *via* unsaturation affect the chain packing ability, which in turn affects the strength of the van der Waals interaction between the unsaturated chains. Thus, the greater the number of unsaturated bonds in the hydrocarbon chain, the lesser the ability of the chains to pack in an ordered fashion, and thus the thermal stability of both the thermotropic and lyotropic phases formed will decrease. Furthermore, the oleoyl derivative is the only member of the unsaturated C18 diethanolamide family capable of forming a crystalline solid. The ability of the amphiphile to crystallize indicates that the oleoyl chain is still able to pack in a somewhat regular fashion thus imparting a solid crystalline structure to the neat oleoyl diethanolamide at lower temperatures. In contrast, the multiple unsaturated bonds in the linoleoyl and linolenoyl derivatives prevent crystalline packing resulting in a smectic liquid crystalline form at low temperatures. This is in contrast to the crystalline solid formed by both the neat unsaturated C18 monoethanolamide amphiphiles[30] and the neat unsaturated C18 urea amphiphiles.[25]

Both the urea and monoethanolamide headgroups exhibit very strong hydrogen bonding, when contrasted with the van der Waals interaction that exists between the hydrocarbon

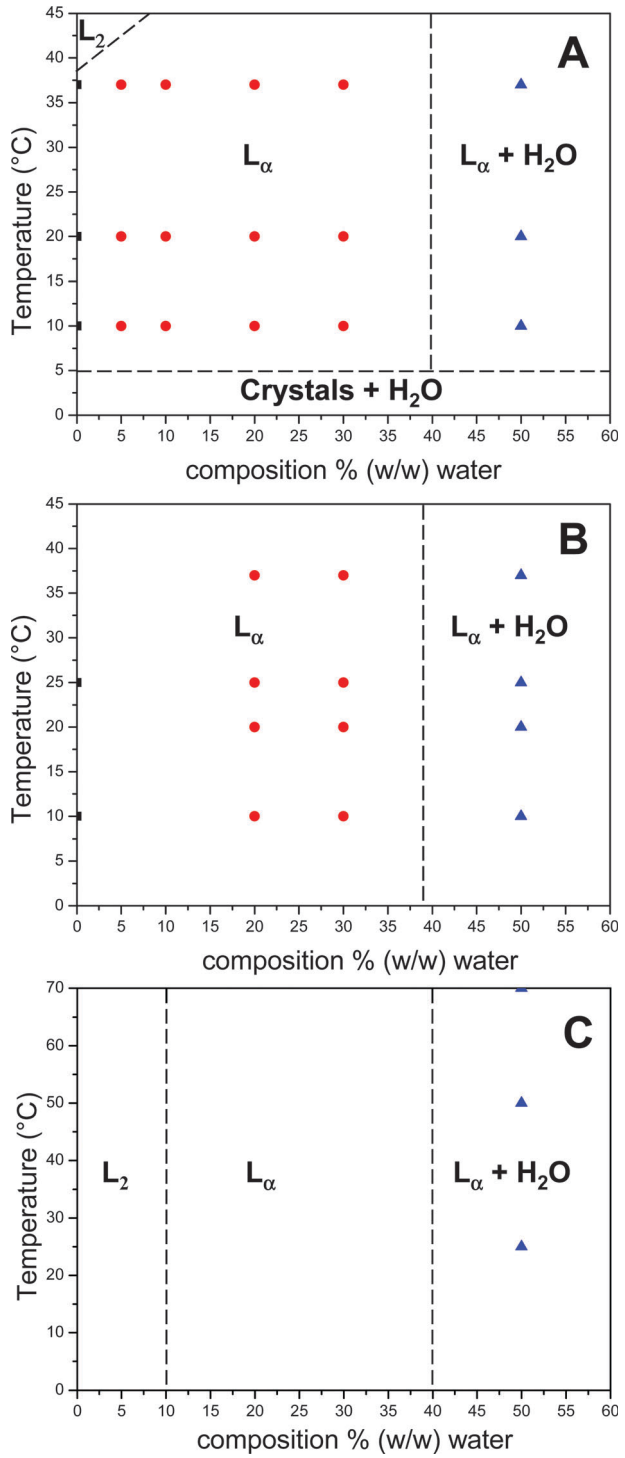

Fig. 9 (A) Partial phase diagram for the oleoyl diethanolamide–water system showing results from SAXS experiments and from polarising microscopy. SAXS results show a smectic phase (■), a fluid lamellar (L_α) phase (●) and a fluid lamellar phase co-existing with excess water (▲). Regions indicated by polarising microscopy indicated include a crystalline phase region, a fluid isotropic inverse micellar L_2 phase, a fluid lamellar phase region, and a region of fluid lamellar phase co-existing with excess water. (B) Partial phase diagram for the linoleoyl diethanolamide–water system showing results from SAXS experiments and from polarizing microscopy. SAXS results show a smectic phase (■), a fluid lamellar (L_α) phase (●) and a fluid lamellar phase co-existing with excess water (▲). A fluid lamellar phase region, including the excess water point is indicated by Polarizing microscopy. (C) Partial phase diagram for the linolenoyl ethanolamide- water system showing results from SAXS experiments and from polarizing microscopy. SAXS results at 50 wt% water show a fluid lamellar phase co-existing with excess water (▲). Regions indicated by polarising microscopy include a fluid isotropic inverse micellar L_2 phase and a fluid lamellar phase. As a guide to the eye, dotted lines demarcate the various phase regions; these should not be considered as true thermodynamic phase boundaries.

moieties.[25,30] These results indicate that the strength of the H-bonding compared to the strength of other intermolecular interactions has a major effect on a molecule's ability to form thermotropic liquid crystalline phases. In the case of the unsaturated C18 diethanolamides, the role of H-bonding and van der Waals interactions within the molecular arrangement are more balanced than those in either their urea or monoethanolamide counterparts. A similar result was seen in a series of hexaalkoxytriphenylenes where the addition of either an amide or urea group in the alkoxy tail resulted in suppression of liquid crystalline behavior in the polymer due to strong hydrogen bonding.[61] Thus, when the stronger interactions within an amphiphile dominate over the weaker ones then the tendency to form liquid crystal mesophases is markedly reduced.

Conclusions

The current study has characterized the thermotropic and lyotropic liquid crystalline behavior of a series of unsaturated C18 diethanolamide amphiphiles. These molecules exhibit amphitropic behavior forming both a lyotropic lamellar phase in the presence of water and a thermotropic smectic liquid crystalline phase when neat. The effective molecular rod-like geometry of this amphiphile family directs the packing ability of the individual molecules in favor of bilayer structures with the hydrophilic and hydrophobic portions of the molecules segregated both in the presence and absence of water. The intricate balance between headgroup H-bonding and interchain van der Waals interaction is key to the phase behavior exhibited by this amphiphile family. Additionally, the degree of unsaturation plays a major role in both the lyotropic and thermotropic phase transition temperatures. As the number of unsaturated bonds increase, the temperature at which both the lyotropic and thermotropic transitions occur decreases. Unsaturation disrupts molecular packing *via* stiff kinks present in the hydrocarbon chain at the unsaturation sites. It is an effective method of increasing chain volume and disrupting intermolecular interactions thereby resulting in alterations to the thermotropic and/or lyotropic liquid crystalline phase behavior of an amphiphile. Here, the unsaturated C18 diethanolamides possess the proper balance of intermolecular forces combined with the necessary geometrical constraints to exhibit amphitropic behavior. By gaining a better understanding of how subtle molecular changes affect both neat and lyotropic phase behavior, the rational design of amphiphiles with properties tailored to a desired application can be targeted.

Acknowledgements

Part of this research was undertaken on the SAXS/WAXS beamline at the Australian Synchrotron, Victoria, Australia. SMS and CEC were the recipients of CSIRO post-doctoral fellowships. CJD was the recipient of an Australian Research Council Federation Fellowship.

References

1 H. L. Sanders, *J. Am. Oil Chem. Soc.*, 1958, **35**, 548–551.
2 M. E. Wittekin and J. H. Benedict, *J. Am. Oil Chem. Soc.*, 1967, **44**, 645–647.
3 Z. G. Xu, D. L. Liu, W. H. Qiao, Z. S. Li and L. B. Cheng, *Pet. Sci. Technol.*, 2006, **24**, 1363–1370.
4 K. J. Liu, A. Nag and J. F. Shaw, *J. Agric. Food Chem.*, 2001, **49**, 5761–5764.
5 T. X. Liu and P. A. Stansly, *Pest Manage. Sci.*, 2000, **56**, 861–866.
6 S. T. Keera and M. A. Deyab, *Colloids Surf., A*, 2005, **266**, 129–140.
7 J. Feng, C. Rodriguez, T. Izawa, H. Kunieda and T. Sakai, *J. Dispersion Sci. Technol.*, 2004, **25**, 163–172.
8 R. O. Brito, E. F. Marques, P. Gomes, M. J. Araujo and R. Pons, *J. Phys. Chem. B*, 2008, **112**, 14877–14887.
9 J. N. Israelachvili, D. J. Mitchell and B. W. Ninham, *J. Chem. Soc., Faraday Trans. 2*, 1976, **72**, 1525–1568.
10 V. Luzzati, A. Tardieu, T. Gulikkrz, E. Rivas and F. Reisshus, *Nature*, 1968, **220**, 485.
11 J. M. Seddon, *Biochim. Biophys. Acta*, 1990, **1031**, 1–69.
12 T. Kaasgaard and C. J. Drummond, *Phys. Chem. Chem. Phys.*, 2006, **8**, 4957–4975.
13 J. Briggs and M. Caffrey, *Biophys. J.*, 1994, **66**, 1263–1263.
14 J. Clogston, J. Rathman, D. Tomasko, H. Walker and M. Caffrey, *Chem. Phys. Lipids*, 2000, **107**, 191–220.
15 L. de Campo, A. Yaghmur, L. Sagalowicz, M. E. Leser, H. Watzke and O. Glatter, *Langmuir*, 2004, **20**, 5254–5261.
16 C. Fong, D. Wells, I. Krodkiewska, P. G. Hartley and C. J. Drummond, *Chem. Mater.*, 2006, **18**, 594–597.
17 C. Fong, D. Wells, I. Krodkiewska, A. Weerawardeena, J. Booth, P. G. Hartley and C. J. Drummond, *J. Phys. Chem. B*, 2007, **111**, 10713–10722.
18 S. S. Funari, M. C. Holmes and G. J. T. Tiddy, *J. Phys. Chem.*, 1992, **96**, 11029–11038.
19 Y. Misquitta and M. Caffrey, *Biophys. J.*, 2001, **81**, 1047–1058.
20 H. Qiu and M. Caffrey, *Chem. Phys. Lipids*, 1999, **100**, 55–79.
21 H. Qiu and M. Caffrey, *Biomaterials*, 2000, **21**, 223–234.
22 S. M. Sagnella, C. E. Conn, I. Krodkiewska, M. Moghaddam and C. J. Drummond, *J. Phys. Chem. B*, 2010, **114**, 1729–1737.
23 H. Takahashi, A. Matsuo and I. Hatta, *Phys. Chem. Chem. Phys.*, 2002, **4**, 2365–2370.
24 J. M. Walsh and G. J. T. Tiddy, *Langmuir*, 2003, **19**, 5586–5594.
25 D. Wells, C. Fong and C. J. Drummond, *J. Phys. Chem. B*, 2006, **110**, 12660–12665.
26 X. J. Gong, S. M. Sagnella and C. J. Drummond, *Int. J. Nanotechnol.*, 2008, **5**, 370–392.
27 D. Wells, C. Fong, I. Krodkiewska and C. J. Drummond, *J. Phys. Chem. B*, 2006, **110**, 5112–5119.
28 D. Wells and C. J. Drummond, *Langmuir*, 1999, **15**, 4713–4721.
29 S. M. Sagnella, C. E. Conn, I. Krodkiewska and C. J. Drummond, *Soft Matter*, 2009, **5**, 4823–4834.
30 S. M. Sagnella, C. E. Conn, I. Krodkiewska, M. Moghaddam, J. M. Seddon and C. J. Drummond, *Langmuir*, 2010, **26**, 3084–3094.
31 S. Z. Mohammady, M. Pouzot and R. Mezzenga, *Biophys. J.*, 2009, **96**, 1537–1546.
32 J. M. Seddon, A. M. Squires, C. E. Conn, O. Ces, A. J. Heron, X. Mulet, G. C. Shearman and R. H. Templer, *Philos. Trans. R. Soc. London, Ser. A*, 2006, **364**, 2635–2655.
33 P. J. Linstrom and W. G. E. Mallard, *National Institute of Standards and Technology*, Gaithersburg, MD, 2005.
34 E. L. Skau, R. R. Mod, J. A. Harris and D. Mitcham, *J. Chem. Eng. Data*, 1980, **25**, 88–89.
35 O. Turpeinen, *J. Am. Chem. Soc.*, 1938, **60**, 56–57.
36 E. S. Lutton, *J. Am. Oil Chem. Soc.*, 1965, **42**, 1068.
37 B. J. Boyd, C. J. Drummond, I. Krodkiewska and F. Grieser, *Langmuir*, 2000, **16**, 7359–7367.
38 S. A. Galema, J. Engberts and H. A. vanDoren, *Carbohydr. Res.*, 1997, **303**, 423–434.
39 B. F. B. Silva and E. F. Marques, *J. Colloid Interface Sci.*, 2005, **290**, 267–274.
40 M. Tokita, S. Funaoka and J. Watanabe, *Macromolecules*, 2004, **37**, 9916–9921.
41 C. A. Ericsson, L. C. Ericsson, V. Kocherbitov, O. Soderman and S. Ulvenlund, *Phys. Chem. Chem. Phys.*, 2005, **7**, 2970–2977.
42 C. A. Ericsson, L. C. Ericsson and S. Ulvenlund, *Carbohydr. Res.*, 2005, **340**, 1529–1537.
43 C. Fong, A. Weerawardena, S. M. Sagnella, X. Mulet, I. Krodkiewska, J. Chong and C. J. Drummond, *Langmuir*, 2011, **27**, 2317–2326.

44 C. Fong, A. Weerawardena, S. M. Sagnella, X. Mulet, L. Waddington, I. Krodkiewska and C. J. Drummond, *Soft Matter*, 2010, **6**, 4727–4741.
45 X. J. Gong, M. J. Moghaddam, S. M. Sagnella, C. E. Conn, S. Danon, L. J. Waddington and C. J. Drummond, *App. Mater. Interfaces*, 2011, in press.
46 V. Kocherbitov and O. Soderman, *Langmuir*, 2004, **20**, 3056–3061.
47 M. J. Moghaddam, L. de Campo, L. J. Waddington and C. J. Drummond, *Soft Matter*, 2010, **6**, 5915–5929.
48 X. Mulet, T. Kaasgaard, C. E. Conn, L. J. Waddington, D. F. Kennedy, A. Weerawardena and C. J. Drummond, *Langmuir*, 2010, **26**, 18415–18423.
49 S. M. Sagnella, C. E. Conn, I. Krodkiewska, X. Mulet and C. Drummond, *Soft Matter*, 2011, **7**, 5319–5328.
50 S. M. Sagnella, X. J. Gong, M. J. Moghaddam, C. E. Conn, K. Kimpton, L. J. Waddington, I. Krodkiewska and C. J. Drummond, *Nanoscale*, 2011, **3**, 919–924.
51 T. Inoue, Y. Hisatsugu, R. Ishikawa and M. Suzuki, *Chem. Phys. Lipids*, 2004, **127**, 161–173.
52 T. Inoue, Y. Hisatsugu, R. Yamamoto and M. Suzuki, *Chem. Phys. Lipids*, 2004, **127**, 143–152.
53 S. Ueno, A. Miyazaki, J. Yano, Y. Furukawa, M. Suzuki and K. Sato, *Chem. Phys. Lipids*, 2000, **107**, 169–178.
54 F. Giesselmann, R. Germer and A. Saipa, *J. Chem. Phys.*, 2005, **123**.
55 J. M. Seddon, R. H. Templer and R. L. a. E. Sackmann, in *Handbook of Biological Physics*, North-Holland, 1995, vol. 1, Part 1, pp. 97–160.
56 C. M. Paleos and D. Tsiourvas, *Curr. Opin. Colloid Interface Sci.*, 2001, **6**, 257–267.
57 S. T. Hyde, in *Handbook of Applied Surface and Colloid Chemistry*, John Wiley & Sons, New York, 2001, pp. 299–332.
58 F. B. Rosevear, *J. Am. Oil Chem. Soc.*, 1954, **31**, 628–639.
59 C. Tschierske, *Curr. Opin. Colloid Interface Sci.*, 2002, **7**, 355–370.
60 C. M. Paleos and D. Tsiourvas, *Angew. Chem., Int. Ed. Engl.*, 1995, **34**, 1696–1711.
61 W. Pisula, Z. Tomovic, M. Wegner, R. Graf, M. J. Pouderoijen, E. W. Meijer and A. Schenning, *J. Mater. Chem.*, 2008, **18**, 2968–2977.
62 S. M. Sagnella, C. E. Conn, I. Krodkiewska and C. J. Drummond, *Phys. Chem. Chem. Phys*, submitted.